Toxicology Letters 180 (2008) 222–229

Contents lists available at ScienceDirect

Toxicology Letters

journal homepage: www.elsevier.com/locate/toxlet

Oxidative stress and apoptosis induced by titanium dioxide nanoparticles in cultured BEAS-2B cells

Eun-Jung Park[a], Jongheop Yi[b], Kyu-Hyuck Chung[c], Doug-Young Ryu[d], Jinhee Choi[e], Kwangsik Park[a,*]

[a] College of Pharmacy, Dongduk Women's University, 23-1, Wolgok-dong, Seongbuk-gu, Seoul 136-714, Republic of Korea
[b] School of Chemical and Biological Engineering, Seoul National University, 599 Gwanangno, Gwanak-gu, Seoul 151-742, Republic of Korea
[c] College of Pharmacy, Sungkyunkwan University, #300, Cheoncheon-dong, Jangan-gu, Suwon 440-746, South Korea
[d] College of Veterinary Medicine, Seoul National University, 599 Gwanangno, Gwanak-gu, Seoul 151-742, Republic of Korea
[e] Faculty of Environmental Engineering, College of Urban Science, University of Seoul, 90 Jeonnong-dong, Dongdaemun-gu, Seoul 130-743, Republic of Korea

ARTICLE INFO

Article history:
Received 27 April 2008
Received in revised form 31 May 2008
Accepted 24 June 2008
Available online 10 July 2008

Keywords:
Titanium dioxide nanoparticles
Apoptosis
Oxidative stress
BEAS-2B cells

ABSTRACT

As the applications of industrial nanoparticles are being developed, the concerns on the environmental health are increasing. Cytotoxicities of titanium dioxide nanoparticles of different concentrations (5, 10, 20 and 40 μg/ml) were evaluated in this study using a cultured human bronchial epithelial cell line, BEAS-2B. Exposure of the cultured cells to nanoparticles led to cell death, reactive oxygen species (ROS) increase, reduced glutathione (GSH) decrease, and the induction of oxidative stress-related genes such as heme oxygenase-1, thioredoxin reductase, glutathione-*S*-transferase, catalase, and a hypoxia inducible gene. The ROS increase by titanium dioxide nanoparticles triggered the activation of cytosolic caspase-3 and chromatin condensation, which means that titanium dioxide nanoparticles exert cytotoxicity by an apoptotic process. Furthermore, the expressions of inflammation-related genes such as interleukin-1 (IL-1), interleukin-6 (IL-6), interleukin-8 (IL-8), TNF-a, and C-X-C motif ligand 2 (CXCL2) were also elevated. The induction of IL-8 by titanium dioxide nanoparticles was inhibited by the pre-treatment with SB203580 and PD98059, which means that the IL-8 was induced through p38 mitogen-acitvated protein kinase (MAPK) pathway and/or extracellular signal (ERK) pathway. Uptake of the nanoparticles into the cultured cells was observed and titanium dioxide nanoparticles seemed to penetrate into the cytoplasm and locate in the peri-region of the nucleus as aggregated particles, which may induce direct interactions between the particles and cellular molecules, to cause adverse biological responses.

1. Introduction

Recently, nanoparticles are issues in many fields such as industrial applications, environmental studies and human health impacts, due to their unique physical and chemical characteristics (Oberdorster et al., 2005; Priestly et al., 2007). In the industrial fields, nanomaterials made from metals such as titanium, silver, gold, cerium, and aluminum have been widely used for commercial purposes. Because of its high stability, anticorrosiveness, and photocatalytic properties, titanium dioxide in nanoparticle form may be one of the most important materials for photocatalysts (Sun et al., 2004), cosmetics, and pharmaceuticals (Gelis et al., 2003). With the increased applications of titanium dioxide nanoparticles, the concerns about their potential human toxicity and their environmental impact have also been increased. The implementation of a systematic process for identifying the environmental health impact of nanoparticles has become an emerging issue for both the industries and the governmental regulatory authorities. Therefore, the development and commercial uses of engineered nanomaterials will present additional challenges for companies and governments in ensuring the safety of products for workers and ultimately, consumers (Warheit et al., 2007a).

Regarding the toxicity of titanium dioxide nanoparticles, lungs seemed to be the main target organ for toxicity studies. When mice were treated with a single intratracheal instillation of 0.1 mg titanium dioxide nanoparticles, the lungs showed significant changes in morphology and histology, including disruption of the alveolar septa, alveolar enlargement (emphysematous change), type II pneumocyte proliferation, increased alveolar epithelial thickness, and the accumulation of particle-laden macrophages (Chen et al., 2006). In another report, mice inhaled acutely at low (0.77 mg/m^3)

* Corresponding author. Tel.: +82 2 940 4522; fax: +82 2 940 4159.
E-mail address: kspark@dongduk.ac.kr (K. Park).

0378-4274/$ – see front matter © 2008 Elsevier Ireland Ltd. All rights reserved.
doi:10.1016/j.toxlet.2008.06.869

or high (7.22 mg/m^3) concentrations of titanium dioxide nanoparticles, and were then necropsied immediately after the exposure. By the inhalation, the numbers of total cells as well as the numbers of macrophages were found to be significantly increased in the bronchoalveolar lavage (BAL) fluid of the mice (Grassian et al., 2007). When rats were intratracheally instilled with a dose of 1 mg/kg or 5 mg/kg of different types of titanium dioxide nanoparticles and the lungs evaluated for BAL fluid inflammatory markers and cell proliferation, the results demonstrated that exposure to titanium dioxide nanoparticles could produce lung inflammation, cytotoxicity, cell proliferation, and histopathological responses, with differential pulmonary effects based upon their composition and crystal structure (Warheit et al., 2007a). Furthermore, the size–effect of titanium dioxide nanoparticles was investigated. Generally, it has been known that nano-sized particles are more toxic than larger particles at identical mass concentration (Oberdorster et al., 2005; Lam et al., 2004). However, in the study of pulmonary instillation with titanium nanoscale rods and dots in rats, toxicity was not dependent upon the particle size or the surface area (Warheit et al., 2007b; Wittmaack, 2007). These findings run counter to the postulation that surface area is a major factor associated with the pulmonary toxicity of nanoscale particles types. Recently, the acute toxicity and biodistribution of titanium dioxide particles in mice after oral administration was reported (Wangs et al., 2007). In the study, titanium dioxide nanoparticles were mainly accumulated in the liver, kidney, spleen, and lung. This means that titanium dioxide nanoparticles could be transported to the lung after uptake by the gastrointestinal tract, and that the lung may be a major target of toxicity following both inhalation and oral administration.

A few studies showed that titanium dioxide nanoparticles induced inflammation in the lung in the absence of ultraviolet (UV) irradiation (Chen et al., 2006; Grassian et al., 2007; Warheit et al., 2007a). Titanium dioxide nanoparticles in the absence of photoactivation-induced oxidative deoxyribonucleic acid (DNA) damage, lipid peroxidation, and micronuclei formation and they increased hydrogen peroxide and nitric oxide production in human bronchial epithelial cells (Gurr et al., 2005). They also resulted in micronuclei formation and apoptosis in Syrian hamster embryo fibroblasts (Rahman et al., 2002). However, the induction of oxidative stress by titanium dioxide nanoparticles and the triggering of mechanisms of oxidative stress due to inflammation and/or apoptotic process have not been elucidated.

In the present work, we evaluated the cytotoxic effect of titanium dioxide nanoparticles using a BEAS-2B cell line derived from human bronchial epithelial normal cells. Furthermore, reactive oxygen species (ROS) generation, intracellular reduced glutathione (GSH) levels, caspase-3 activity, chromosomal condensation, gene expressions as markers of oxidative stress and/or inflammation were also investigated to reveal possible mechanisms of cell death induced by exposure to titanium dioxide nanoparticles.

2. Materials and methods

2.1. Materials

Commercial titanium dioxide nanoparticles (P-25, 21-nm size) were purchased from Degussa Korea (Incheon, Korea). A BEAS-2B cell line, derived from human bronchial epithelial cells, was purchased from the American Type Culture Collection (ATCC) (Manassas, VA, USA). DMEM/F12 media were purchased from GIBCO Invitrogen (Seoul, Korea). 3-(4,5-Dimethylthiazol-2-yl)-2,5-diphenyltetrazolium bromide (MTT), dichlorofluorescein diacetate (DCFH-DA), 4′,6-diamidino-2-phenylindole (DAPI), reduced glutathione and orthophthaldialdehyde were purchased from Sigma–Aldrich (St. Louis, MO, USA). The caspase-3 assay kit was purchased from R&D systems Inc. (Minneapolis, MN, USA). The RNA isolation kit (RNAgents®) was purchased from the Promega Company (Madison, WI, USA). The AccuPower RT/PCR Premix for the amplification of nucleic acid was purchased from Bioneer (Daejeon, Korea).

2.2. Cell culture and nanoparticle treatment

BEAS-2B cells were maintained in Dulbecco's-modified Eagle's medium (DMEM)/F12 containing 10% FBS, penicillin 100 IU/ml, and streptomycin 100 μg/ml. Cells were grown and maintained in 28 cm^2 cell culture flasks at 37 °C in a 5% CO_2 humidified incubator. The test suspension of titanium dioxide nanoparticles was prepared using the culture media and dispersed for 20 min by using a sonicator (Branson Inc., Danbury, CT, USA) to prevent aggregation. The cells were treated with various concentrations of particles according to the time schedule which is designated in the following section of each toxicological study.

2.3. Cell viability test

Cell viability was measured by the MTT assay. Cells were seeded on 96-well tissue culture plates with 5×10^3 to 2×10^4 cells in 100 μl media per well. After a 24-h stabilization of the cells, nanoparticle suspension 100 μl (10, 20, 40 and 80 μg/ml concentrations) was added to the cell media respectively, to make final concentrations of 5, 10, 20, and 40 μg/ml. Cells were exposed to the nanoparticles for 24, 48, 72, and 96 h, respectively. At the end of exposure, 40 μl of MTT solution (2 mg/ml) was added and the cells were incubated for 4 h at 37 °C. Cells were treated with 150 μl of dimethylsulfoxide (DMSO) and absorbance was quantified at 540 nm using the microplate spectrophotometer system (VersaMax, Molecular Devices, Sunnyvale, CA, USA). The viability of the treated group was expressed as a percentage of non-treated control group, which was assumed to be 100%.

2.4. Measurement of ROS and GSH

To measure ROS generation, a fluorometric assay using intracellular oxidation of DCFH-DA was performed (Elbekai and El-Kadi, 2005; Fotakis et al., 2005). Cells grown to confluence at 24 h after seeding were pre-treated with different concentrations (5, 10, 20 and 40 μg/ml) of nanoparticles for 24 h, washed with phosphate-buffered saline (PBS), and then incubated with 40 μM DCFH-DA for 30 min. At the end of DCFH-DA incubation, cells were washed with PBS, lysed with NaOH, and aliquots were transferred to a black well plate. Then, the fluorescence of dichlorofluoroscein (DCF), which is the oxidized product of DCFH-DA, was measured using a microplate spectrofluorometer (GeminiXPS, Molecular Devices, Sunnyvale, CA, USA) with excitation and emission wavelengths of 485 nm and 530 nm, respectively. Protein assay was performed using the Lowry assay. For the visual image of ROS generation, the cells were cultured in the presence or absence of titanium dioxide nanoparticles (10, 20 and 40 μg/ml), washed with PBS, and then loaded with 40 μM DCFH-DA for 30 min. The fluorescence in cells was visualized using a fluorescence microscope (Nikon, Tokyo, Japan) with an excitation of 485 nm and an emission of 530 nm, and an exposure time of 1/100 to 1/130 s.

To investigate the relationship between the increased ROS and the level of antioxidant materials in cells, the intracellular GSH level was determined (Elbekai and El-Kadi, 2005; Fotakis et al., 2005). The cells treated with nanoparticles (5, 10, 20 and 40 μg/ml) in six-well plates for 24 h were washed with PBS, and 1% perchloric acid was added to the cell pellet and left for 10 min on ice. The cell lysates were centrifuged at 13,000 rpm at 4 °C for 5 min prior to analysis in order to remove precipitated protein. Cell lysates, KH_2PO_4/EDTA buffer, and *o*-phthaldialdehyde were put in black 96-well plates and incubated in the dark at room temperature for 30 min. Fluorescence was measured using a fluorescence multi-well plate reader with excitation and emission wavelengths of 350 nm and 420 nm, respectively (Hissin and Hilf, 1976). Results were calculated as nmol of glutathione per mg of protein and presented as a percentage of the control group. Protein assays in the cell lysate were performed using a bicinconinic acid (BCA) protein assay kit (Pierce, Rockford, IL, USA).

2.5. Caspase-3 activity

The activity of caspase-3 was determined using a colorimetric assay kit. Briefly, cells were incubated with different concentrations of nanoparticles (5, 10, 20 and 40 μg/ml) for 24 h. The cells were first lysed by the solution provided in the assay kit to collect their intracellular contents. The cell lysates could then be tested for their enzyme activity by the addition of a caspase-specific peptide that is conjugated to the color reporter molecule, *p*-nitroaniline (*p*NA). The cleavage of the peptide by the caspase, releases the chromophore *p*NA, which can be quantitated spectrophotometrically at 450 nm. Protein assays in the cell lysate were performed using a BCA protein assay kit (Pierce, Rockford, IL, USA).

2.6. DAPI staining for chromosome condensation

To evaluate chromosome condensation, DAPI staining was performed. The DAPI solution was applied to cultured cells in chamber slides (10, 20 and 40 μg/ml), and the slides were incubated for 10 min in the dark at 37 °C, and the images of the nucleus were made by a fluorescence microscope (Nikon, Tokyo, Japan) with an excitation of 330–380 nm and an emission of 420 nm, and an exposure time of 1/100 to 1/130 s (Dhar-Mascareno et al., 2005).

Table 1
Primer sequences of oxidative stress-related genes used in this study

Gene name	GB No.	Primer sequences
Glutathione-*S*-transferase	NM146421.1	F: 5′-CCATCTTTGAGAACACAGGT-3′ R: 5′-GAGAAGATTCGTGTGGACAT-3′
Heme oxygenase-1	NM002133.1	F: 5′-CTCTGAAGTTTAGGCCATTG-3′ R: 5′-AGTTGCTGTAGGGCTTTATG-3′
Thioredoxin reductase	NM182742.1	F: 5′-AAACCAATACCAGCAAGAAA-3′ R: 5′-CTATGAGAATGCTTATGGGC-3′
Catalase	NM001752.2	F: 5′-TCATGACATTTAATCAGGCA-3′ R: 5′-GTGTCAGGATAGGCAAAAAG-3′
Hypoxia inducible gene	NM001530.2	F: 5′-GAGCATTCTGCAAAGCTAGT-3′ R: 5′-ATTGATTGCATCTCCATCTC-3′
Interleukin 1	BC039733.1	F: 5′-TTTTAGTGCCTGCATTTGGG-3’ R: 5′-TCTCCACCCACCACAAACAC-3′
Interleukin 6	M14584.1	F: 5′-CCAGTACCCCCAGGAGAAGA-3′ R: 5′-TTGTTTTCTGCCAGTGCCTC-3’
Interleukin 8	M28130.1	F: 5′-ACCGGAAGGAACCATCTCAC-3′ R: 5′-AGTTTTCCTTGGGGTCCAGA-3’
TNF-alpha	AL157444.1	F: 5′-GGGCTTAAGGGTGTCTGAGC-3′ R: 5′-CAAAGAAGTTCCTGGCCTCC-3′
C-X-C motif ligand 2 (CXCL2)	BC015753.1	F: 5′-CCACACTCAAGAATGGGCAG-3′ R: 5′-TGGTCAGTTGGATTTGCCAT-3′
Actin	NM001101.2	F: 5′-GGCGGACTATGACTTAGTTG-3′ R: 5′-AAACAACAATGTGCAATCAA-3′

2.7. Gene expression analysis

Gene expression analysis was evaluated in a concentration-dependent and a time-dependent manner. For the preparation of total ribonucleic acid (RNA), the RNA isolation kit (RNAgents®) was used according to the manufacturer's instructions. Reverse-transcription polymerase chain reaction (reverse-transcription (RT)-PCR) was performed using oligo deoxythymidine primer in 20-μl volumes at 42 °C for 60 min. The RT-PCR reaction was done with 1 μg of total RNA, 1 μl of 20-μM oligo dT primer, and 18 μl of reaction mixture which was provided by *AccuPower* RT/PCR PreMix. Then PCR was performed in a 20-μl total mixture volume for 25–28 cycles at 95 °C for 1 min, 55 °C for 1 min, and 72 °C for 1 min. Amplified cDNA products were separated on 1.5% agarose gel by electrophoresis. The primer sequences of amplified genes are shown in Table 1. Actin mRNA was also amplified and shown to be a loading control.

2.8. Nanoparticle uptake test

Cultured cells were treated with a 40 μg/ml concentration of titanium dioxide nanoparticles. The cells were kept in the CO_2 incubator and taken out from the incubator for microscopic observation using a phase-contrast microscope (200×) at 0.5, 3, and 24 h after treatment, respectively.

2.9. Statistical analysis

The results of cell viability, ROS generation, GSH level, and caspase-3 activity are presented as the mean ± standard deviation (S.D.) of three or four separate experiments. The results of the chemically treated groups were compared to those of the non-treated control group and represented as the percentage of the control value. The values were compared using the Student's *t*-test, and levels of significance were presented for each result.

3. Results

3.1. Cytotoxicity

To examine the toxic effects of titanium dioxide nanoparticles, BEAS-2B cells were incubated with different concentrations (5, 10, 20 and 40 μg/ml) of nanoparticles and viability was determined 24, 48, 72, and 96 h after treatment, respectively. As shown in Fig. 1, cell viability was decreased by treatment with nanoparticles in both a time- and concentration-dependent manner.

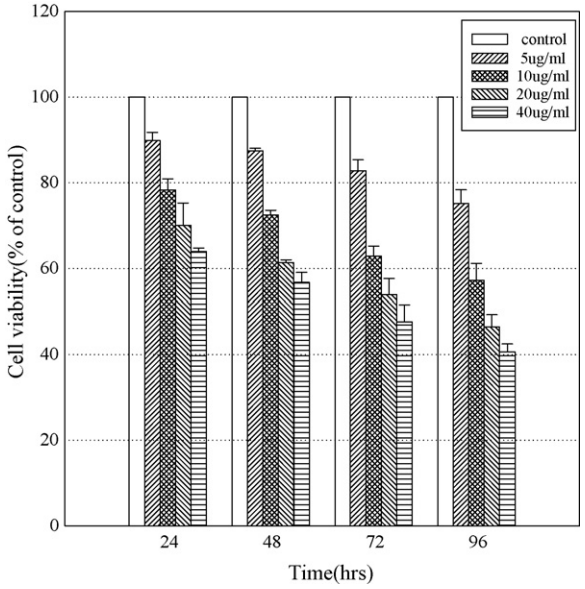

Fig. 1. Effects of titanium dioxide nanoparticles on the viability of BEAS-2B cells. Cell viability was assessed by MTT assays and results are presented as a percentage of control group viability. Cells (5×10^3 to 2×10^4 cells) were treated with the indicated concentrations of titanium dioxide nanoparticles for 24, 48, 72, and 96 h for concentration-dependent tests. Cell viability was greatly reduced in a concentration-dependent and time-dependent manner by nanoparticle exposure. All treated groups showed statistically significant differences from the control group by the Student's *t*-test ($p < 0.01$). Results represent the means of three separate experiments, and error bars represent the standard error of the mean.

3.2. ROS generation and GSH reduction

The fluorescence intensity of oxidized DCF was increased in BEAS-2B cells when treated with nanoparticles as shown in Fig. 2. This means that ROS generation was occurring in response to the

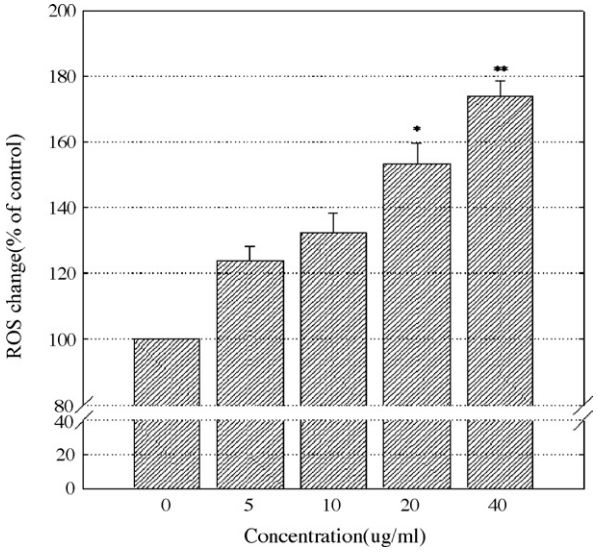

Fig. 2. Effects of titanium dioxide nanoparticles on ROS induction in BEAS-2B cells. Cells grown in confluence were treated with nanoparticles of designated concentrations for 24 h, washed with phosphate-buffered saline, and then incubated with 40 μM DCFH-DA. At the end of DCFH-DA incubation, the cells were lysed with NaOH and the fluorescence of an aliquot was measured. Results represent the means of three separate experiments, and error bars represent the standard error of the mean. Treated groups (20 μg/ml and 40 μg/ml) showed statistically significant differences from the control group by the Student's *t*-test (*$p < 0.05$; **$p < 0.01$). Data were represented as the percentage of the ROS level in the control group.

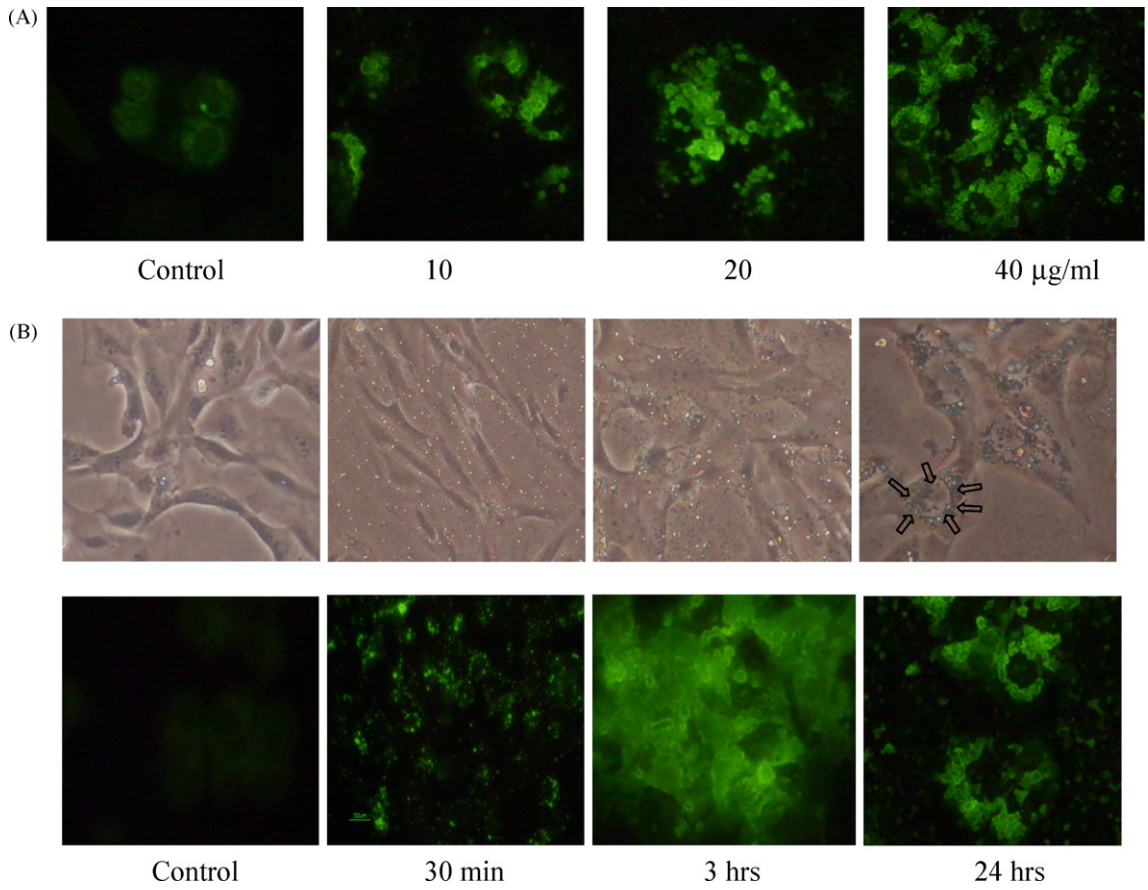

Fig. 3. Microscopic images of ROS generation by titanium dioxide nanoparticles using DCFH-DA staining. (A) Cells were cultured in the presence of nanoparticles (10, 20 and 40 μg/ml), washed with PBS, and then loaded with 40 μM DCFH-DA. After being washed with PBS, cells were visualized by a fluorescence microscope (200×). (B) In upper panel, cellular uptake and aggregation of titanium dioxide nanoparticles were observed by inverted microscope without treatment with DCFH-DA. Titanium dioxide nanoparticles were localized in the peri-region of nuclei. The images of aggregates were enlarged with the increase of exposure time, to form a ring-like shape. Arrows show the aggregates of titanium dioxide nanoparticles in the cells. In lower panel, ROS images were shown. Cells were treated with 40 μg/ml concentration of nanoparticles for 30 min, 3 h, and 24 h, respectively and then loaded with 40 μM DCFH-DA. After being washed with PBS, cells were visualized by a fluorescence microscope (200×).

treatment with titanium dioxide nanoparticles. Visualization of ROS generation with the fluorescence microscope showed that oxidized DCF fluorescence was increased in the cells cultured in the presence of titanium dioxide nanoparticles (10, 20 and 40 μg/ml) in a concentration- and time-dependent manner, while fluorescence was insignificant in the control group (Fig. 3A and B). The induction of ROS was correlated with the amount and position of titanium dioxide nanoparticles which entered the cells (Fig. 3B). In Fig. 4, decreased levels of GSH were also shown in the nanoparticle-treated group in a concentration-dependent manner. The level of intracellular GSH in the treated group with 40 μg/ml seemed to be about 60% of the control group at 24-h exposure.

3.3. *mRNA expression of oxidative stress- and inflammation-related genes*

To investigate the expression level of each mRNA related to the oxidative stress or the inflammation responses in BEAS-2B cells, RT-PCR was performed. As shown in Fig. 5A, when the cells were treated with nanoparticles (5, 10, 20 and 40 μg/ml) for 3 h, various oxidative stress-related genes including heme oxygenase-1, thioredoxin reductase, glutathione-*S*-transferase, catalase and hypoxia inducible gene were shown to be induced. Heme oxygenase-1, which is a well-known biomarker of oxidative stress, seemed to be induced maximally by the exposure of 3 h or 4 h, but the induction was decreased as the exposure-time extended to 24 h (Fig. 5B). The expression of the inflammation-related genes such as interleukin-1 (IL-1), interleukin-6 (IL-6), interleukin-8 (IL-8), TNF-a, and C-X-C motif ligand 2 (CXCL2) were also increased as shown in Fig. 6A by the exposure to nanoparticles (5, 10, 20 and 40 μg/ml) for 3 h. Time course of inflammation-related gene induction was shown in Fig. 6B. Induction of mRNA expression was shown as early as 1-h exposure. When the exposure-time was extended to 24 h, the induction level was decreased to the control level after maximal induction around 4 h exposure. The housekeeping gene, actin was not changed by nanoparticle treatment. To evaluate the induction mechanism of IL-8, inhibitors of IL-8 gene expression were used. As shown in Fig. 7, the induction of IL-8 by titanium dioxide nanoparticles was decreased by pre-treatment of inhibitors of the p38 mitogen-activated protein kinase (MAPK) pathway (SB203580) and of the extracellular signal-regulated kinase (ERK) pathway (PD98059), respectively (Hoffmann et al., 2002).

3.4. *Induction of caspase-3 activity and chromosome condensation*

Caspase-3, which plays a key role in the apoptotic pathway of cells, was increased following the treatment with titanium dioxide nanoparticles (Fig. 8). When cells were treated with 5, 10, 20, and 40 μg/ml concentrations of nanoparticles for 24 h, the activity of caspase-3 was increased even from the lowest concentration

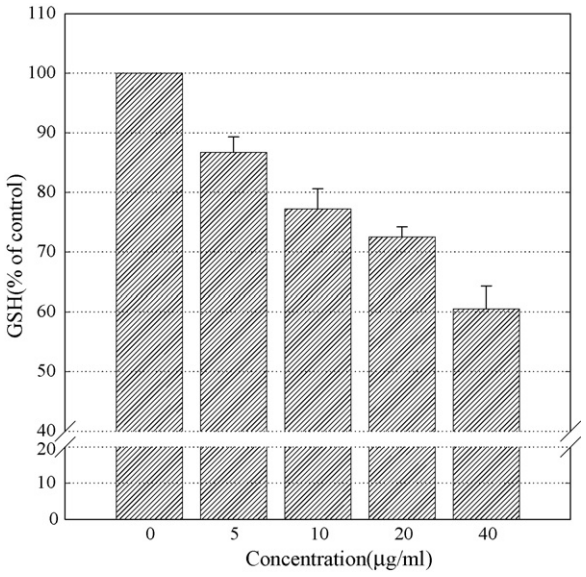

Fig. 4. Effects of titanium dioxide nanoparticles on the level of intracellular-reduced glutathione (GSH). A fluorometric method using *o*-phthaldialdehyde was used to measure GSH. GSH was calculated as nmol of glutathione per mg of protein and then was presented as a percentage of control. Results represent the means of three separate experiments, and error bars represent the standard error of the mean. All groups treated with nanoparticles (5, 10, 20 and 40 μg/ml) showed statistically significant differences by Student's *t*-test from the control group ($p < 0.01$). Data are represented as the percentage of the GSH level in control group.

of 5 μg/ml to the highest concentration of 40 μg/ml. In addition to the caspase-3 activity, chromatin condensation was also evaluated by DAPI staining. When cells were treated with 10, 20, and 40 μg/ml concentrations of titanium dioxide nanoparticles for 24 h, chromatin condensations were observed in the treated group in a concentration-dependent manner (Fig. 9). The caspase-3 activation and chromatin condensation in BEAS-2B suggested that titanium dioxide nanoparticles caused cell death by an apoptotic process.

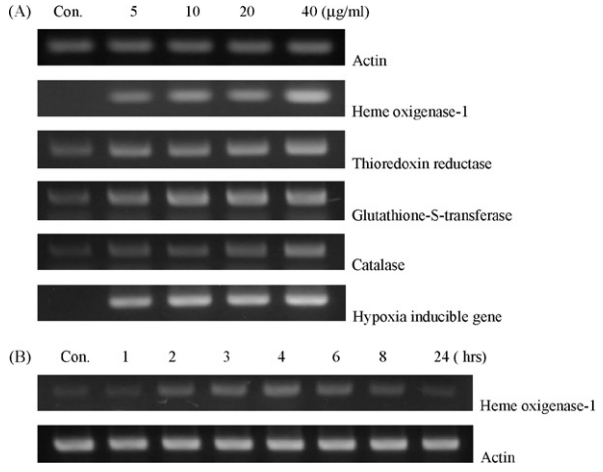

Fig. 5. Effect of titanium dioxide nanoparticles on the induction of oxidative stress-related genes (A) Cells were treated with nanoparticles for 4 h with the indicated exposure concentrations (control, 5, 10, 20 and 40 μg/ml). mRNA transcription was detected by RT-PCR analysis using the respective primers described in Table 1. Results were confirmed by several separate experiments and representative images were shown. (B) Time-course of heme oxygenase-1 induction was shown. Actin mRNA was used as a housekeeping gene.

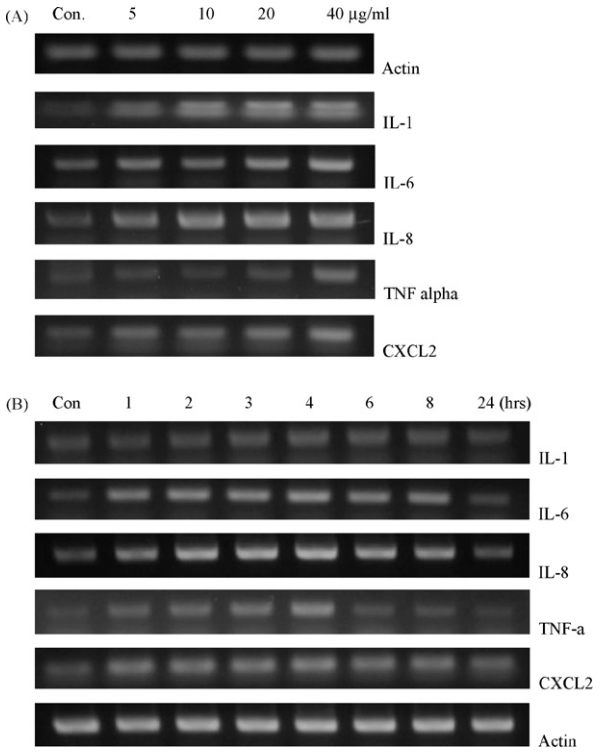

Fig. 6. Effect of titanium dioxide nanoparticles on the induction of inflammation-related genes. (A) Cells were treated with nanoparticles for 4 h with the indicated exposure concentration (control, 5, 10, 20 and 40 μg/ml). mRNA transcripts were detected by RT-PCR using the respective primers described in Table 1. Results were confirmed by several separate experiments and representative images are shown. (B) Time-courses of the inductions of inflammation-related genes are shown. Actin mRNA was used as a housekeeping gene.

4. Discussion

Much evidence of hazardous health effects of nanoparticles has been reported in toxicological studies. Reports on the toxicities of nanoparticles, both in engineered nanomaterials and in naturally occurring particles, are rapidly increasing (Kipen and Laskin, 2005; Kagan et al., 2005; Curtis et al., 2006; Hardman, 2006). As one of the toxic mechanisms of nanoparticles, the generation of ROS seems to be most widely studied. There are some reports that ROS production has been found in the cells treated with C60 fullerenes, SWNTs (single-walled nanotubes), cerium oxide nanoparticles, and other metal particles (Sayes et al., 2005; Hussain et al., 2005; Green and Howman, 2005; Park et al., 2008; Limbach et al., 2007). Nanoparticles may alter ROS production and thereby may cause interference in biological antioxidant defense responses (Xia et al., 2004; Foster et al., 2006). It has been demonstrated that nanoparticles of various

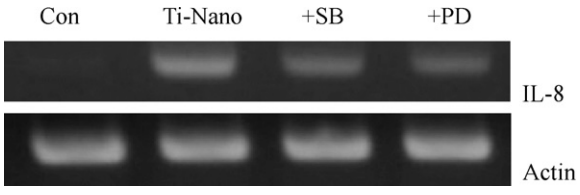

Fig. 7. Effects of SB203580 and PD98059 on the induction of IL-8 by titanium dioxide nanoparticles. SB203580 and PD98059 were pre-treated for 4 h before the treatment with titanium dioxide nanoparticles at 40 μg/ml. mRNA transcription was detected by RT-PCR analysis using the respective primers described in Table 1. Results were confirmed by several separate experiments and representative images were shown. +SB stands for the pre-treatment of SB203580 (2.5 μM) and +PD stands for the pre-treatment of PD98059 (25 μM). Actin mRNA was used as a housekeeping gene.

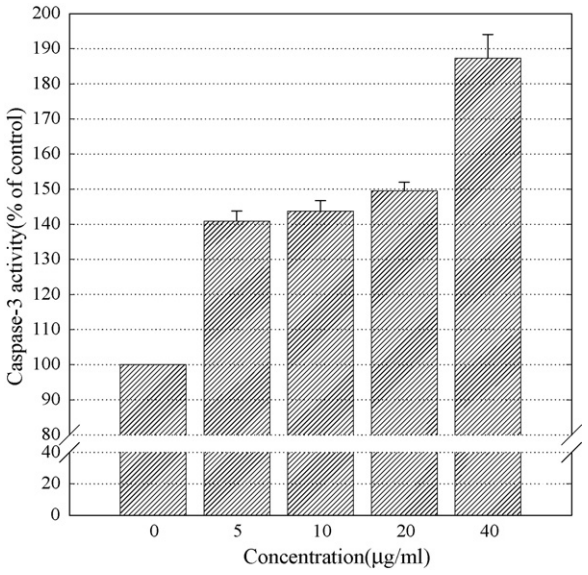

Fig. 8. Effects of titanium dioxide nanoparticles on caspase-3 activity. Cells were treated with the indicated concentration of 10-nm nanoparticles (5, 10, 20 and 40 μg/ml) for 24 h. Caspase-3 activity was measured using a colorimetric caspase-specific substrate. After the reaction, the chromophore *p*NA was determined at 405 nm. Results represent the means of four separate experiments, and error bars represent the standard error of the mean. Statistical significance was shown in all treated groups by the Student's *t*-test ($p < 0.01$).

sizes and different chemical compositions seemed to attack mitochondria, which are redox active organelles. However, the exact mechanisms of ROS generation by nanoparticles are still unclear at this moment.

In this study, the cytotoxicity of titanium dioxide nanoparticles was studied using cultured BEAS-2B cells. Viability was reduced to 40% of the control group in 40 μg/ml treated group and the cytotoxicity was shown even at the lowest concentration of 5 μg/ml (Fig. 1). Oxidative stress was elevated by the treatment with titanium dioxide nanoparticles (Fig. 2). Consequently, cytotoxicity in BEAS-2B cells seemed to be caused by oxidative stress. As shown in Fig. 2, elevation of ROS was concentration-dependent from 5 μg/ml to 40 μg/ml. ROS is an important factor in the apoptotic process, and the excess generation of ROS induces mitochondrial membrane permeability and damages the respiratory chain, to trigger the apoptotic process (Jezek and Hlavata, 2005; Valko et al., 2006). ROS generation was also confirmed using fluorescence microscope in DCFH-DA-treated cells (Fig. 3A and B). The induction level of ROS was correlated with the exposure concentration of nanoparticles (Fig. 3A). As shown in the time-course of ROS generation (Fig. 3B), this reached its highest level by 3 h of exposure and fluorescence was distributed evenly in the cytoplasm. At 24 h after exposure, ROS generation was restricted only in the peri-region of the nuclear membrane, where nanoparticles existed as aggregated forms. It seems that ROS are generated in the place where nanoparticles reside and occur by the direct interactions between nanoparticles and biomolecules in the cells. Furthermore, ROS generation and GSH depletion have been known to be closely related in cultured BEAS-2B cells, as shown in Figs. 2 and 4. This pattern was also shown with cerium oxide nanoparticles (Park et al., 2008). Following the induction of ROS, GSH levels were decreased to 60% of the level of the control group in 40 μg/ml concentration treated group for 24-h exposure. Free radical species generated by titanium dioxide nanoparticles seemed to reduce the levels of cellular antioxidants significantly. Similar effects were observed in the cells treated with nanoparticles such as SWCNTs (single-wall carbon nanotubes), semiconductor quantum dots and cerium oxide

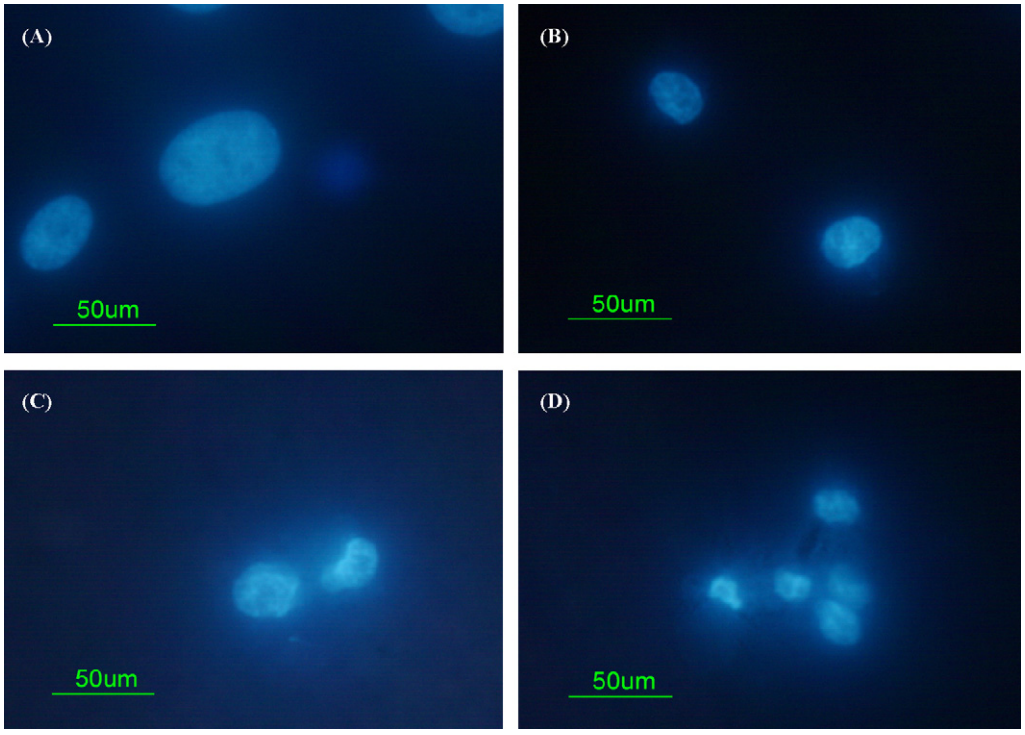

Fig. 9. Increase of chromosome condensation by titanium dioxide nanoparticles with DAPI staining. Cells were treated with the indicated concentrations of titanium dioxide nanoparticles for 24 h. DAPI (4′,6-diamidino-2-phenylindole) staining was performed on control and treated cells. DAPI solution was applied to cultured cells in chamber slides, and the cells were incubated for 10 min in the dark at 37 °C. Images of the nuclei were made using a fluorescence microscope (200×). (A) Control group, (B) 10 μg/ml treated group, (C) 20 μg/ml treated group and (D) 40 μg/ml treated group.

(Li et al., 2006; Chan et al., 2006; Long et al., 2006; Park et al., 2008).

The heme oxygenase-1 which oxidatively cleaves heme to produce biliverdin, is a well-known biomarker of oxidative stress, and was reported to be induced in animal cells by inorganic mercury (Park and Park, 2007). The induction of thioredoxin reductase and catalase are also known to be clear biomarkers of oxidative stress (Hansen et al., 2006; Margonis et al., 2007). It is known that down-regulation of thioredoxin reductase increases the level of oxidized thioredoxin, which is a regulatory apparatus for oxidative injury in mitochondria, and leads to increased susceptibility to cell death (Das, 2005). Oxidative stress may also trigger inflammation signals. By the induction of ROS, expressions of inflammation-related genes such as IL-I, IL-6, IL-8, TNF-a, and CXCL2 were also increased in a concentration-dependent manner (Fig. 6A). As shown in Fig. 5B, heme oxygenase-1 induction was not prolonged by 24 h exposure. The induction pattern of IL-8 and other inflammatory genes seems to be similar to that of heme oxygenase-1. The expression level of inflammation genes such as IL-I, IL-6, IL-8, TNF-a, and CXCL2 were also decreased by an exposure of 24 h. The level of treated group after 24 h was decreased to the control level. It seemed that gene (mRNA) transcription system may have been damaged by generated ROS. Aggregated nanoparticles in the peri-region of nuclear membrane may have blocked the nuclear pores and therefore may have affected the gene transcriptional system.

It is known that IL-8 gene expression is regulated by a combination of three different mechanisms: first, derepression of the gene promoter; second, transcriptional activation of the gene by nuclear factor-kB, Jun N-terminal kinase (JNK), and ERK; third, stabilization of the mRNA by the p38 MAPK pathway. When the cells were pre-treated with an inhibitor of p38 MAPK pathway, SB203580, or an inhibitor of ERK pathway, PD98059, the induction of IL-8 gene expression was decreased (Fig. 7). This means that the level of IL-8 mRNA was increased by exposure to titanium dioxide nanoparticles, by both transcriptionial and post-transcriptional pathway.

The activation of caspase-3 has been known to be triggered by ROS, and many chemicals are known to increase the activity of caspase-3 by ROS. *t*-Butylhydroperoxide generates ROS, and activates caspase-3 to lead to apoptosis (Kanupriya et al., 2007). Nanoscale hydroxyapatite activated caspase-3 and caspase-9 to induce mitochondria-dependent apoptosis in human gastric cancer SGC-7910 cells (Chen et al., 2007) and it has also been shown that magnetic nanoparticles containing 5-fluorouracil (5-FU) induced caspase-3 activity (Wang et al., 2007). It is uncertain whether it is the functional groups on the nanoparticles that are the real active components to activate caspase enzymes or whether it is the nanoparticles themselves. As an example of metal nanoparticles, CdSe quantum dots induced caspase-3 activation and caused apoptosis in human neuroblastoma cells via a mitochondrial-dependent pathway, in which no functional chemical modification was made (Chan et al., 2006). Titanium dioxide nanoparticles in our study also activated caspase-3 and the activity was increased to about 190% of the level of the control group when the cells were treated with 40 μg/ml for 24 h. As is already known, caspase-3 activation may cause chromosome condensation and DNA fragmentation to trigger apoptosis of cells (Porter, 1999). Condensed chromatin and fragmentation was shown in the cells treated with titanium dioxide nanoparticles by DAPI staining in Fig. 9. We do not have direct evidence that the chromatin condensation occurred due to the direct interaction between nanoparticles and chromatin, or through the caspase-3 activation pathway, at this time.

When we treated the cells with nanoparticles and observed the cells using a phase contrast microscope, we found that nanoparticle uptake into the cytoplasm occurred rapidly after treatment, and that the nanoparticles resided mainly around the peri-region of the nuclear membrane, as shown in Fig. 3B (upper panel) at 24-h exposure. The nanoparticles were aggregated mainly in the peri-region of nuclear membrane, not in the cytoplasmic region to interfere the function of endoplasmic reticulumn or to block nuclear pore.

In conclusion, the present study revealed the cytotoxicity of titanium dioxide nanoparticles with the induction of ROS and the decreased level of intracellular GSH in cultured BEAS-2B cells. With the induction of ROS, the expressions of oxidative stress-related genes including heme oxygenase-1 or inflammation-related genes including IL-8 were increased. Cytosolic caspase-3 activation and chromatin condensation were also shown in the cells, which suggested the apoptotic process. The nanoparticles penetrated into the plasma membrane and located in the peri-region of nuclear membranes, which means the particles may have direct interactions with cellular molecules to cause adverse biological responses in cells.

Acknowledgement

This work was supported by the Eco-technopia 21 project of the Korea Ministry of the Environment.

References

Chan, W., Shiao, N., Lu, P., 2006. CdSe quantum dots induce apoptosis in human neuroblastoma cells via mitochondrial-dependent pathways and inhibition of survival signals. Toxicol. Lett. 167, 191–200.
Chen, X., Deng, C., Tang, S., Zhang, M., 2007. Mitochondria-dependent apoptosis induced by nanoscale hydroxyapatite in human gastric cancer SGC-7901 cells. Biol. Pharm. Bull. 30 (1), 128–132.
Chen, H., Su, S., Chien, C., Lin, W., Yu, S., Chou, C., Chen, J., Yang, P., 2006. Titanium dioxide nanoparticles induce emphysema-like lung injury in mice. FASEB J. 20, 2393–2395.
Curtis, J., Greenberg, M., Kester, J., Phillips, S., Krieger, G., 2006. Nanotechnology and nanotoxicology: a primer for clinicians. Toxicol. Rev. 25 (4), 245–260.
Das, K.C., 2005. Thioredoxin and its role in premature newborn biology. Antioxid. Redox. Signal. 7, 1740–1743.
Dhar-Mascareno, M., Carcamo, J.M., Golde, D.W., 2005. Hypoxia-reoxygenation-induced mitochondrial damage and apoptosis in human endothelial cells are inhibited by vitamin C. Free Radic. Biol. Med. 38, 1311–1322.
Elbekai, R.H., El-Kadi, A.O.S., 2005. The role of oxidative stress in the modulation of aryl hydrocarbon receptor-regulated genes by As^{3+}, Cd^{2+}, and Cr^{6+}. Free Radic. Biol. Med. 39, 1499–1511.
Foster, K.A., Galeffi, F., Gerich, F.J., Turner, D.A., Muller, M., 2006. Optical and pharmacological tools to investigate the role of mitochondria during oxidative stress and neurodegeneration. Prog. Neurobiol. 79, 136–171.
Fotakis, G., Cemeli, E., Anderson, D., Timbrell, J.A., 2005. Cadmium chloride-induced DNA and lysosomal damage in a hepatoma cell line. Toxicol. In Vitro 19, 481–489.
Gelis, C., Girard, S., Mavon, A., Delverdier, M., Pailous, N., Vicendo, P., 2003. Assessment of the skin photoprotective capacities of an organo-mineral broad-spectrum sunblock on two ex vivo skin models. Photodermatol. Photoimmunol. Photomed. 19 (5), 242–253.
Grassian, V.H., O'Shaughnessy, P.T., Adamcakova-Dodd, A., Pettibone, J.M., Thorne, P.S., 2007. Inhalation exposure study of titanium dioxide nanoparticles with a primary particle size of 2 to 5 nm. Environ. Health Perspect. 115 (3), 397–402.
Green, M., Howman, E., 2005. Semiconductor quantum dots and free radical induced DNA nicking. Chem. Commun. 121, 121–123.
Gurr, J.R., Wang, A.S., Chen, C.H., Jan, K.Y., 2005. Ultrafine titanium dioxide particles in the absence of photoactivation can induce oxidative damage to human bronchial epithelial cells. Toxicology 213 (1–2), 66–73.
Hansen, J.M., Zhang, H., Hones, D.P., 2006. Differential oxidation of thioredoxin-1, thioredoxin-2, and glutathione by metal ions. Free Radic. Biol. Med. 40, 138–145.
Hardman, R., 2006. A toxicological review of quantum dots: toxicity depends on physicochemical and environmental factors. Environ. Health Perspect. 114 (2), 165–172.
Hissin, P.J., Hilf, R., 1976. Fluorometric method for determination of oxidized and reduced glutathione in tissues. Anal Biochem. 74, 214–226, J. Leukocyte Biol., 72, 1976, 847–855.
Hoffmann, E., Dittrich-Breiholz, O., Holtmann, H., Kracht, M., 2002. Multiple control of interleukin-8 gene expression. J. Leukocyte Biol. 72 (5), 847–855.
Hussain, S.M., Hess, K.L., Gearhart, J.M., Geiss, K.T., Schlager, J.J., 2005. In vitro toxicity of nanoparticles in BRL 3A rat liver cells. Toxicol. In Vitro 19, 975–983.
Jezek, P., Hlavata, L., 2005. Mitochondria in homeostasis of reactive oxygen species in cell, tissues, and organism. Int. J. Biochem. Cell Biol. 37, 2478–2503.
Kagan, V.E., Bayer, H., Shvedova, A.A., 2005. Nanomedicine and nanotoxicology: two sides of the same coin. Nanomedicine 1 (4), 313–316.

Kanupriya, Prasad, D., Ram, M.S., Sawhney, R.C., Ilavazhagan, G., Banerjee, P.K., 2007. Mechanism of *tert*-butylhydroperoxide induced cytotoxicity in U-937 macrophages by alteration of mitochondrial function and generation of ROS. Toxicol. In Vitro 21, 846–854.

Kipen, H.M., Laskin, D.L., 2005. Smaller is not always better: nanotechnology yields nanotoxicology. Am. J. Physiol. Lung Cell Mol. Physiol. 289, L696–L697.

Lam, C., James, J.T., McCluskey, R., Hunter, R.L., 2004. Pulmonary toxicity of single-wall carbon nanotubes in mice 7 and 90 days after intratracheal instillation. Toxicol. Sci. 77, 126–134.

Li, Z., Hulderman, T., Salmen, R., Chapman, R., Leonard, S.S., Young, S., Shvedova, A., Luster, M.I., Simeonova, P.P., 2006. Cardiovascular effects of pulmonary exposure to single-wall carbon nanotubes. Environ. Health Perspect. 115, 377–382.

Limbach, L.K., Wick, P., Manser, P., Grass, R.N., Bruinink, A., Stark, W.J., 2007. Exposure of engineered nanoparticles to human lung epithelial cells: influence of chemical composition and catalytic activity on oxidative stress. Environ. Sci. Technol. 41 (11), 4158–4163.

Long, T.C., Saleh, N., Tilton, R.D., Lowry, G.V., Veronesi, B., 2006. Titatnium dioxide (P25) produces reactive oxygen species in immortalized brain microglia (BV2): implications for nanoparticle neurotoxicity. Environ. Sci. Technol. 40 (14), 4346–4352.

Margonis, K., Fatouros, I.G., Jamurtas, A.Z., Kikolaidis, M.G., Douroudos, I., Chatzinikolaou, A., Mitrakou, A., Mastorakos, G., Papassotiriou, I., Taxildaris, K., Kouretas, D., 2007. Oxidative stress biomarkers responses to physical overtraining: Implications for diagnosis. Free Radic. Biol. Med. 43, 901–910.

Oberdorster, G., Oberdoster, E., Oberdorster, J., 2005. Nanotoxicology: an emerging discipline evolving from studies of ultrafine particles. Environ. Health Perspect. 113 (7), 823–829.

Park, E.J., Park, K., 2007. Induction of reactive oxygen species and apoptosis in BEAS-2B cells by mercuric chloride. Toxicol. In Vitro 21, 789–794.

Park, E.J., Choi, J., Park, Y., Park, K., 2008. Oxidative stress induced by cerium oxide nanoparticles in cultured BEAS-2B cells. Toxicology 245 (1–2), 90–100.

Porter, A.G., 1999. Protein translocation in apoptosis. Trends Cell Biol. 9, 394–401.

Priestly, B.G., Harford, A.J., Rsim, M.R., 2007. Nanotechnology: a promising new technology-but how safe? Med. J. Aust. 186, 187–188.

Rahman, Q., Lohani, M., Dopp, E., Pemsel, H., Jonas, L., Weiss, D.G., Schiffmann, D., 2002. Evidence that ultrafine titanium dioxide induces micronuclei and apoptosis in Syrian hamster embryo fibroblasts. Environ. Health Perspect. 110 (8), 797–800.

Sayes, C.M., Gobin, A.M., Ausman, K.D., Mendez, J., West, J.L., Colvin, V.L., 2005. Nano-C60 cytotoxicity is due to lipid peroxidation. Biomaterials 26, 7587–7595.

Sun, D., Meng, T.T., Loong, H., Hwa, T.J., 2004. Removal of natural organic matter from water using a nano-structured photocatalyst coupled with filtrating membrane. Water Sci. Technol. 49, 103–110.

Valko, M., Rhodes, C.J., Moncol, J., Izakovic, M., Mazur, M., 2006. Free radicals, metals and antioxidants in oxidative stress-induced cancer. Chem. Biol. Interact. 160, 1–40.

Wang, J.M., Xiao, B.L., Zheng, J.W., Chen, H.B., Zou, S.O., 2007. Effect of targeted magnetic nanoparticles containing 5-FU on expression of bcl-2, bax and caspase 3 in nude mice with transplanted human liver cancer. World J. Gastroenterol. 13 (23), 3171–3175.

Wangs, J., Zhou, G., Chen, C., Yu, H., Wans, T., Ma, Y., Jia, G., Gao, Y., Li, B., Sun, J., Li, Y., Jiao, F., Zhao, Y., Chai, Z., 2007. Acute toxicity and biodistribution of different sized titanium dioxide particles in mice after oral administration. Toxicol. Lett. 168, 176–185.

Warheit, D.B., Borm, P.J., Hennes, C., Lademann, J., 2007a. Testing strategies to establish the safety of nanomaterials: conclusion of an ECETOC workshop. Inhal. Toxicol. 19 (8), 631–643.

Warheit, D.B., Hoke, R.A., Finlay, C., Donner, E.M., Reed, K., Sayes, C.M., 2007b. Development of a base set of toxicity tests using ultrafine TiO_2 particles as a component of nanoparticles risk management. Toxicol. Lett. 171, 99–110.

Wittmaack, K., 2007. In search of the most relevant parameter for quantifying lung inflammatory response to nanoparticle exposure: particle number, surface area, or what? Environ. Health Perspect. 115 (2), 187–194.

Xia, T., Korge, P., Weiss, J.N., Li, N., Venkatesen, M.I., Sioutas, C., Nel, A., 2004. Quinones and aromatic chemicals compounds in particulate matter induce mitochondrial dysfunction: implications for ultrafine particle toxicity. Environ. Health Perspect. 112, 1347–1358.